Developmental Biology 405 (2015) 173–181

Contents lists available at ScienceDirect

Developmental Biology

journal homepage: www.elsevier.com/locate/developmentalbiology

Genomes & Developmental Control

Natural variation of the expression pattern of the segmentation gene *even-skipped* in *melanogaster*

Pengyao Jiang [a,*], Michael Z. Ludwig [a,b], Martin Kreitman [a,b], John Reinitz [a,b,c,d]

[a] Department of Ecology & Evolution, University of Chicago, IL 60637, USA
[b] Institute for Genomics & Systems Biology, Chicago, IL 60637, USA
[c] Department of Statistics, University of Chicago, IL 60637, USA
[d] Department of Molecular Genetics and Cell Biology, University of Chicago, IL 60637, USA

ARTICLE INFO

Article history:
Received 29 October 2014
Received in revised form
23 June 2015
Accepted 24 June 2015
Available online 27 June 2015

Keywords:
Drosophila melanogaster
even-skipped
Intraspecific variation
Quantitative biology
Deletion polymorphism
knirps

ABSTRACT

The evolution of canalized traits is a central question in evolutionary biology. Natural variation in highly conserved traits can provide clues about their evolutionary potential. Here we investigate natural variation in a conserved trait—*even-skipped* (*eve*) expression at the cellular blastoderm stage of embryonic development in *Drosophila melanogaster*. Expression of the pair-rule gene *eve* was quantitatively measured in three inbred lines derived from a natural population of *D. melanogaster*. One line showed marked differences in the spacing, amplitude and timing of formation of the characteristic seven-striped pattern over a 50-min period prior to the onset of gastrulation. Stripe 5 amplitude and the width of the interstripe between stripes 4 and 5 were both reduced in this line, while the interstripe distance between stripes 3 and 4 was increased. Engrailed expression in stage 10 embryos revealed a statistically significant increase in the length of parasegment 6 and a decrease in the length of parasegments 8 and 9. These changes are larger than those previously reported between *D. melanogaster* and *D. pseudoobscura*, two species that are thought to have diverged from a common ancestor over 25 million years ago. This line harbors a rare 448 bp deletion in the first intron of *knirps* (*kni*). This finding suggested that reduced Kni levels caused the deviant *eve* expression, and indeed we observed lower levels of Kni protein at early cycle 14A in L2 compared to the other two lines. A second of the three lines displayed an approximately 20% greater level of expression for all seven *eve* stripes. The three lines are each viable and fertile, and none display a segmentation defect as adults, suggesting that early-acting variation in *eve* expression is ameliorated by developmental buffering mechanisms acting later in development. Canalization of the segmentation pathway may reduce the fitness consequences of genetic variation, thus allowing the persistence of mutations with unexpectedly strong gene expression phenotypes.

1. Introduction

Waddington (1942) introduced the idea of canalization, which involves the conservation of phenotype in the presence of extensive genetic and environmental variation. The extent to which genetic variation can be buffered is currently unknown. Moreover, it is unclear if a canalized trait is maintained over evolution by phenotypically neutral mutations or a series of small compensatory phenotypic changes (Martinez et al., 2014; Bullaughey, 2011). The conservation of gene expression driven by enhancers from highly diverged species (Hare et al., 2008; Fisher et al., 2006; Romano and Wray, 2003; Barrière et al., 2011; Ludwig et al., 1998) shows that functional conservation does not require sequence conservation, but these observations shed little light on the detailed process of evolutionary change which conserved the phenotype. *Trans* changes in the above process complicate matters further, and hence have received little attention. Natural variation acts on extant individuals, and therefore can reveal limits on developmental constraints and provide clues about the evolutionary potential of a conserved trait. Here we investigate natural variation in a conserved trait, the formation of the seven-striped pattern of *even-skipped* (*eve*) RNA expression at the blastoderm stage of embryonic development in *Drosophila melanogaster*.

eve is one of the most well-characterized genes in *D. melanogaster*. It is essential for the formation of segments (Nüsslein-Volhard et al., 1980), and while classified as a pair-rule gene, it has the unique property that null mutations lead to a complete abolition of segments (Macdonald et al., 1986). The segmentation function of *eve* is executed in the blastoderm stage of embryonic development. Transcripts can be reliably detected by cleavage

* Corresponding author.
E-mail address: pyjiang@uchicago.edu (P. Jiang).

http://dx.doi.org/10.1016/j.ydbio.2015.06.019
0012-1606/

cycle 12 and protein by cleavage cycle 13. After the 13th nuclear division, protein and RNA expression refine from a single broad domain to a characteristic pattern of seven transverse stripes (Surkova et al., 2008; Fowlkes et al., 2011). These dynamic changes in expression are a consequence of the activation of *eve* expression by broadly distributed maternal factors and its repression by more localized domains of zygotic gap gene expression (Stanojevic et al., 1991; Reinitz and Sharp, 1995). *eve* is necessary for the correct initiation of the expression of the segment polarity gene *engrailed* (*en*), which stably demarcates the future parasegmental borders (Gilbert, 2003).

The seven-stripe pattern of *eve* before gastrulation is conserved in the suborder Brachycera (Davis and Patel, 2002), albeit with different subcellular localizations in different species (Bullock et al., 2004). Within the genus *Drosophila*, the dynamic pattern of *eve* expression in *Drosophila pseudoobscura* is very similar to that of *D. melanogaster* despite the fact that these species diverged 25–55 million years ago (Fowlkes et al., 2011; Richards et al., 2005).

The individual enhancers of *eve* are very well characterized in terms of function (Harding et al., 1989; Goto et al., 1989; Small et al., 1992, 1993, 1996; Arnosti et al., 1996; Fujioka et al., 1999; Janssens et al., 2006; Kim et al., 2013). A 15 kb segment of DNA (−6.4 kb to +8.6 kb of *eve*) can provide a normal segmentation phenotype and rescue an *eve* null mutant to hatching (Fujioka et al., 1999, 2002). If the stripe 2 enhancer is deleted from the construct, *eve* stripe 2 is greatly reduced in amplitude with a short parasegment 3 and vestigial En stripe 4, a lethal phenotype (Ludwig et al., 2005). Other stripes have effects on survival that are marked but less severe. Transforming *eve* null flies with the *eve* locus bearing a deletion of the 4+6 enhancer results in viable flies missing certain abdominal segments (Fujioka et al., 2002). The viability of these transformants may be a consequence of residual 4+6 expression driven from outside the classical enhancer, but it is equally possible that non-terminal abdominal segments are not absolutely required for viability.

Previous studies on the intraspecific variation of *eve* expression involved quantitative measurements of stripe placement but not amplitude in three lines of flies with differing egg size. *eve* expression among these lines scaled with egg size, demonstrating that intraspecific egg size variation can be compensated for by expression variation (Lott et al., 2007). This point was reinforced by an experiment to artificially select for small or large embryos. In this case, the proportionality of *eve* stripe spacing to embryo length was not preserved, providing crucial evidence that *eve* stripe placement can be variable (Miles et al., 2011). In both examples the phenotype under study was egg size, a complex genetic trait, with its consequences for *eve* expression a secondary effect. For this reason, the phenotypic alterations in these lines have not yet been fully mapped to sequence. In contrast, there exist two well-characterized small deletions of the *D. melanogaster* *eve* *cis*-regulatory region in natural populations, but evidence linking them to phenotypic changes is ambiguous (Palsson et al., 2014).

In this work we characterize intraspecific variation in *eve* expression in terms of quantitative expression level, position, and timing. Our analysis of the three lines, while providing only a glimpse of the full range of *eve* phenotypic variation, demonstrates that significant quantitative variation exists, and can be provisionally assigned to specific changes in sequence.

2. Results

2.1. The dynamics of eve expression in three D. melanogaster lines

For reasons unrelated to the findings reported here, we examined *eve* expression in three lines from the Drosophila Genetic Reference Panel (DGRP) (Mackay et al., 2012). These were RAL-437 (denoted as L1 in this work), RAL-502 (L2), and RAL-365 (L5). We unexpectedly found that *eve* expression from L2 differed from that of the other two lines much more strongly than the previously reported *eve* expression differences between *D. melanogaster* and *D. pseudoobscura* (Fowlkes et al., 2011), motivating the analysis presented here.

Image analysis of *eve* gene expression was carried out from 2D confocal scans of laterally oriented embryos fluorescently stained for nuclei, Eve protein, and *eve* RNA. These scans were transformed into quantitative data at cellular resolution by image segmentation. The embryos were categorized into eight different time classes (T1–T8), each about 6.5 mins long during cell cycle 14A (Surkova et al., 2008). Background staining was removed, and 1D data from the central 10% of dorso-ventral values was used for the detection of quantitative features of the expression pattern (Janssens et al., 2005). The analysis of *eve* expression in this paper was based on RNA expression. Protein expression resembles that of RNA with a lag of one time class (Supplementary Figures S1 and S2).

Fig. 1 and Supplementary Figure S1 show the dynamics of *eve* RNA expression from typical individual embryos at each time class in the three lines during cell cycle 14A. The expression dynamics of *eve* in L2 are visibly different from the other two lines. For example, at T3 the presumptive stripes 4–6 are a single expression domain in L2 while L1 and L5 have already formed separate stripes. In T4 and T5, when L1 and L5 have formed 7 stripes, there is little or no stripe 5 *eve* expression in L2. By T6, stripe 5 *eve* expression in L2 rises to the levels seen in other stripes. Moreover, the 3/4 interstripe is wider in L2 than in the other two lines, with stripe 3 expressed at higher levels in L2.

We made a more precise analysis of differences in the *eve* expression patterns of the three lines by performing feature detection on the expression patterns. We performed the analysis on embryos from T4 to T8, because this is the period when reproducible features of the expression pattern can be characterized (Surkova et al., 2008). We made pairwise comparisons on stripe morphology features using the Wilcoxon rank sum test. We performed inference as to whether gene expression differed with respect to each class of feature as follows. There are $n=mk$ individual Wilcoxon tests, performed for each class of feature, where m is the number of such features (e.g. there are 6 interstripes) and k is the number of time classes they are measured in, which in this application is always 5 (T4–T8). After the tests, we did Bonferroni correction of n tests given the significance value of 0.05.

We considered three types of features: stripe height, interstripe width and stripe width (Supplementary Figure S3). Stripe height is measured from the peak of the stripe to the minimum of the adjacent interstripe (Ludwig et al., 2011; Manu et al., 2013). Stripes 2–6 have two such height measurements, corresponding to the two adjacent interstripes; stripes 1 and 7 each has one. The A-P position at a point where expression was midway between stripe peak and interstripe minimum was taken to be location of the stripe border. We generated 6 interstripe distances and 7 stripe width from the 14 border positions.

We first calculated the absolute stripe height in the three lines (Supplementary Figure S4), and found that L5 had higher expression overall than the other two lines. The Wilcoxon rank sum test for pooled L5 stripe height was significantly different from L1 and L2 (in both cases, $p < 2.2 \times 10^{-16}$), while L1 and L2 show more modest differences ($p = 0.045$), which supports our observation (boxplot shown in Supplementary Figure S5). We also did pairwise Wilcoxon rank sum tests for the stripe height at each time class and each position (Supplementary Table S1). As expected, most

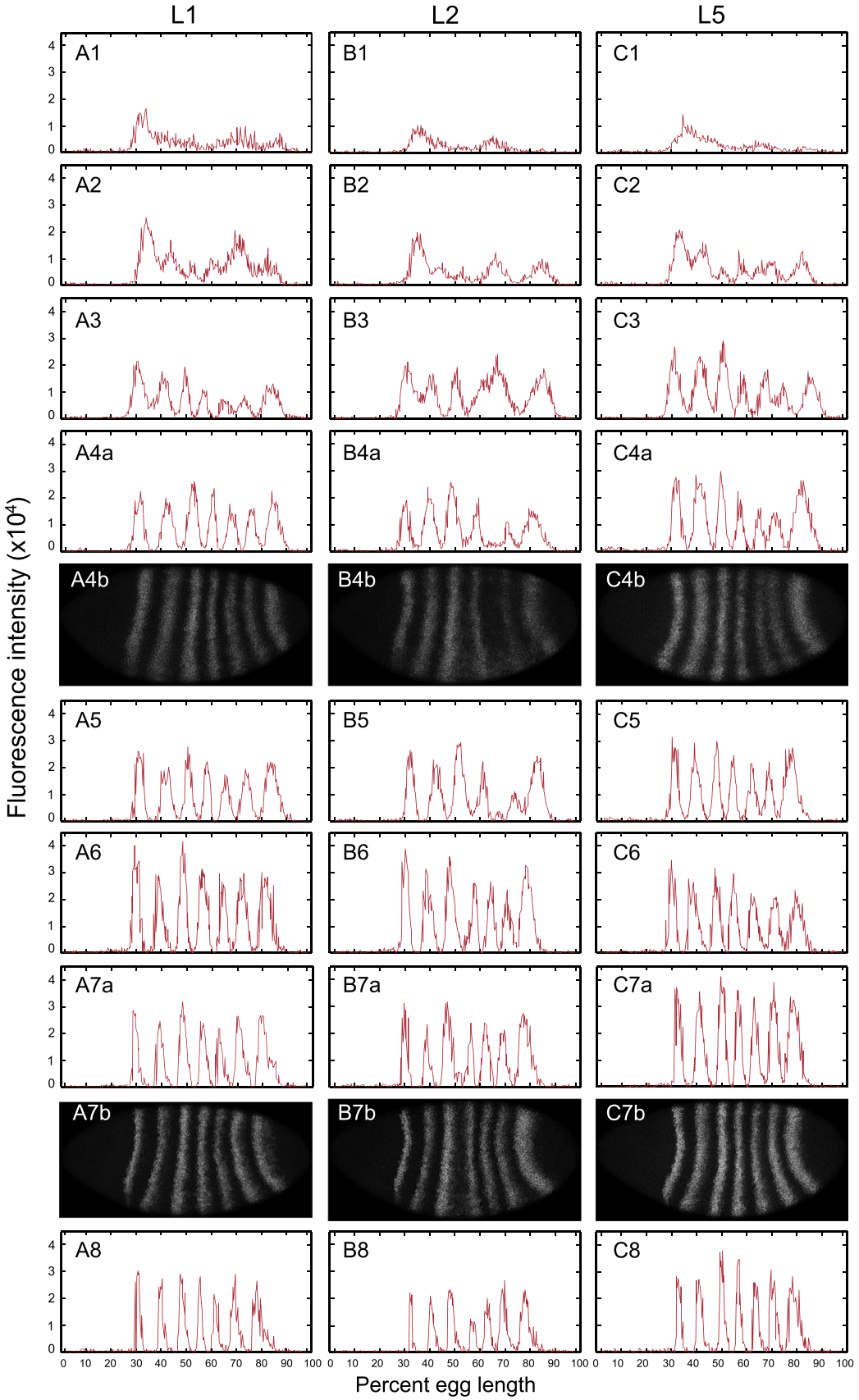

Fig. 1. 1D *eve* RNA expression from single embryo in cycle 14 from 3 lines. Each column shows *eve* RNA expression in one line (A: L1, B: L2, and C: L5). The Arabic number following the letter represents the corresponding time class, T1–T8. Each row shows the *eve* 1D RNA expression in its time class; for T4 and T7 embryos, both 1D expression (indicated by 'a') and the corresponding RNA fluorescent *in situ* embryo image (indicated by 'b') is shown. The expression is from 10% stripe from the middle of laterally oriented embryo after segmentation and background removal.

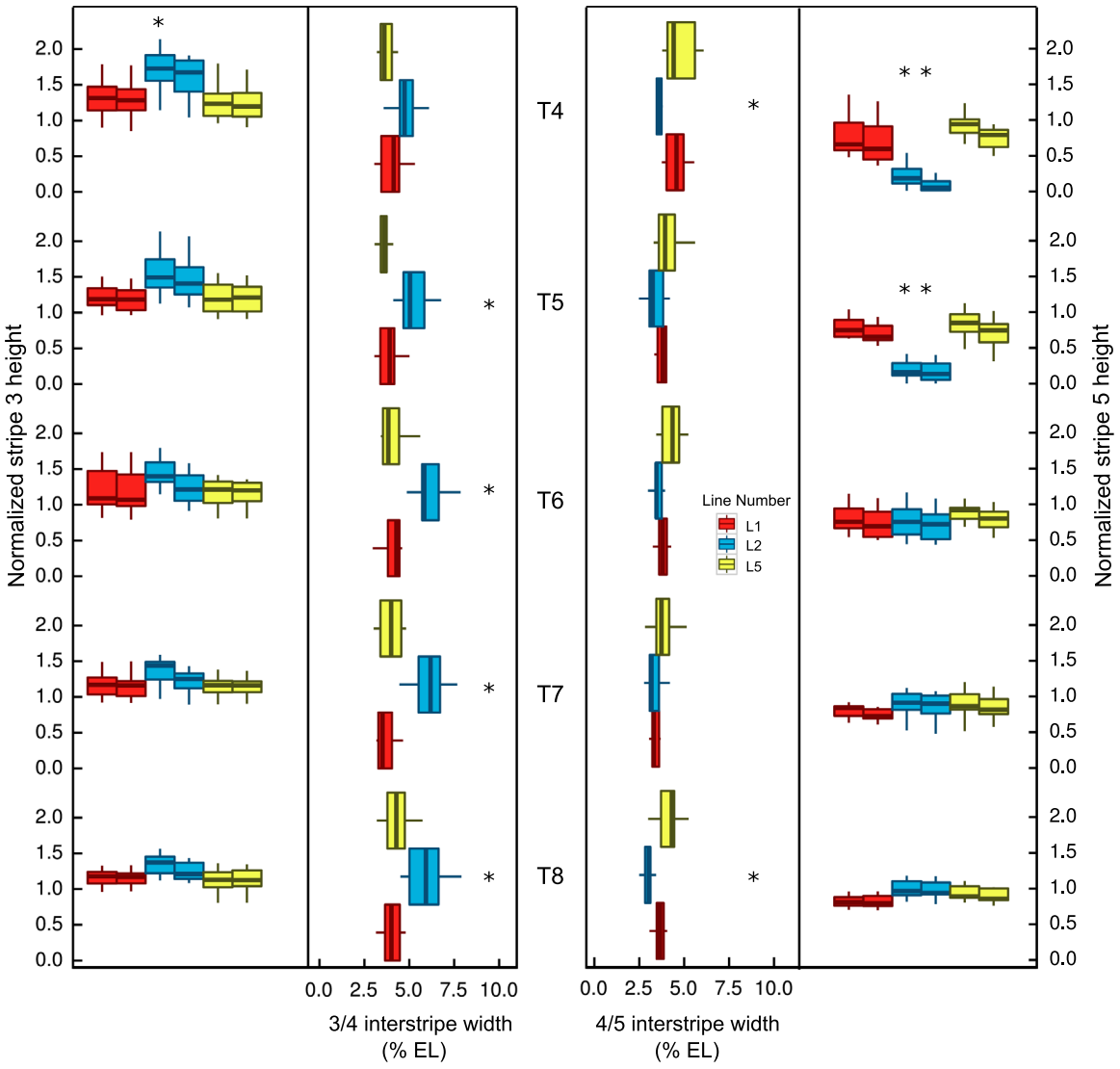

Fig. 2. Quantification of normalized stripe height and interstripe width. Left to right: normalized stripe 3 height, 3/4 interstripe width, 4/5 interstripe width and normalized stripe 5 height from T4 to T8. If a feature is significantly different in two pairwise tests after Bonferroni correction, an asterisk is marked on top of the shared line for that feature. Two boxes represent each height, the one on the left shows the anterior height of the stripe, while the right shows the posterior height of the stripe. Outliers in boxplot are not shown.

differences arose from the higher overall expression in L5. Specifically, for stripe 2 (positions 2 and 3 in the table), L5 is expressed at a significantly higher level than L1 and L2. Notwithstanding this fact, the overall pattern of expression in L5 appeared very similar to L1 by visual inspection (Supplementary Figure S4). In order to compare the features for individual stripes more closely, we normalized stripe height in the three lines by dividing by the mean fluorescence intensity in that line in a given temporal class to detect changes in specific features. After normalizing stripe height, as expected, the most significant differences arose from L2 with respect to L1 and L5 in more specific features (Supplementary Figure S4 and Supplementary Table S2).

The major result from individual tests of quantitative features (Fig. 2 and Supplementary Tables S2–S4) was that L2 has a delay of maturation in stripe 5, with an increase of the 3/4 interstripe width and a decrease of the 4/5 interstripe width as a consequence. Specifically, for normalized stripe height, stripe 3 was significantly higher in L2 than L1 or L5 in T4, while stripe 5 was lower in both T4 and T5 but reached similar levels as the other two by T6. The interstripe distance between stripes 3 and 4 in L2 was significantly wider in T5–T8, and that between 4 and 5 is narrower at T4 and T8 compared to the other two lines (Supplementary Figure S4). Overall, the dynamic *eve* pattern in L1 and L5 resembled that seen in the lab stock Oregon R and Canton S (Surkova et al., 2008; Fowlkes et al., 2011), with that in L2 deviating from this pattern. These results indicate that *eve* expression differs among the individual lines.

Previous studies show that egg length varies within species (Houchmandzadeh et al., 2002; Gregor et al., 2007; Lott et al., 2007; Manu et al., 2009; Miles et al., 2011). Therefore, we measured embryo size for the three lines from confocal-scanned images. Our results show that embryos from L2 have reduced AP axis length and increased DV axis length compared to the other two lines (Supplementary Figure S6). This change of embryo size in L2 could be related to the change of *eve* expression observed in L2, but we did not further address this possible relationship in this work.

2.2. Downstream effect of the eve pattern

We sought to measure the functional effects of these expression differences by assaying expression of *eve*'s functional target,

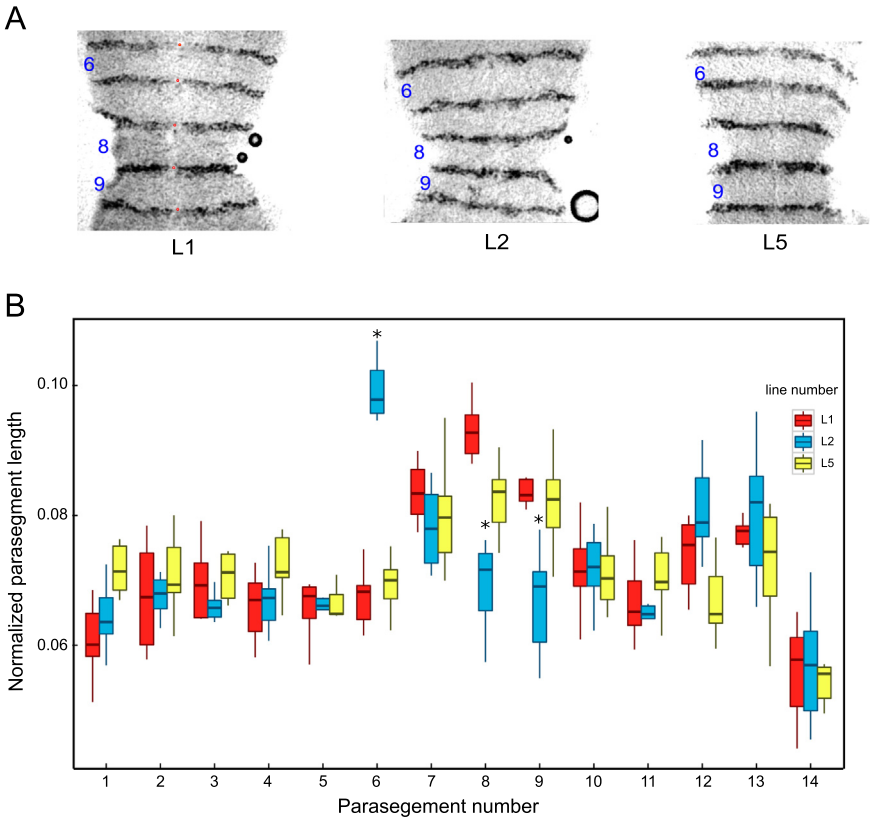

Fig. 3. Normalized parasegment lengths. (A) Images of En expression in parasegments 6–9 of stage 10 dissected embryos from the three lines, as indicated. The red dots mark the anterior of the En stripes demarcating the parasegment. These fiducial marks were used to calculate the length of each parasegment. (B) shows the quantification of the normalized parasegment distance for each line. Significant differences of one line from the other two are marked with an asterisk on the boxplot. Outliers in boxplot are not shown.

en, which is a marker of parasegment boundaries. Stage 10 embryos were stained for En protein (Fig. 3A), and parasegment length was measured as the distance between the anterior margins of two successive En stripes, normalized to the sum of all such lengths. The results of these measurements (Fig. 3B) showed that parasegment 6 is significantly longer while parasegments 8 and 9 are shorter in L2 compared to the two other lines. The alternation of *eve* stripe widths in L2 thus has specific functional consequences.

2.3. Cause of altered expression in L2

We next explored the genetic basis of *eve* expression in L2. Given the marked alterations in stripe 5 expression, we first compared stripe 5 enhancer sequences (Gallo et al., 2011). Sequence alignment (Supplementary Figure S7) revealed 5 SNPs in stripe 5 enhancer among the three lines, one of which is unique in L5. The remaining four SNPs are shared between L2 and L5 but differ with L1. Thus, there is no candidate SNP in the L2 stripe 5 enhancer to potentially account for the aberrant stripe 5 phenotype. For this reason, we consider it unlikely that the SNPs in the stripe 5 enhancer underlie the observed expression changes in L2.

In the absence of obvious differences in the stripe 5 enhancer, we checked the full *eve* sequence and the coding and flanking 2 kb regions of plausible *trans*-regulators among the three lines (Supplementary Table S5) for large deletions (30 bp minimum length) that is unique in L2 (Karolchik et al., 2014). By visualizing the alignment in clustalx (Larkin et al., 2007), we found large deletions or missing data in the DGRP sequences for *eve*, *giant (gt)*, *knirps* (*kni*) and *runt*. Direct experimental checks by PCR revealed that of the four putative deletions, only the one in *kni* is real (Supplementary Table S7. We used BLAT (Kent, 2002) to map back the sequence and found that the deletion is 448 bp in length and lies at the 5′ end of the first intron of *kni* (Supplementary Figure S8).

Several lines of evidence suggest that the deletion in the *kni* intron in L2 could be the cause of the altered *eve* expression. First, in *kni* mutants, only *eve* stripes 4–6 are abolished, while stripes 1–3 and 7 are present in T5–T8 at the protein level, although their amplitude is reduced (Surkova et al., 2013, Figure 1). Second, in *kni* mutant embryos stripe 3 has a larger amplitude than other stripes. Finally, in *kni* heterozygotes, stripe 5 is completely absent until T5 but reaches a level close to wild type level by the onset of gastrulation (Frasch and Levine, 1987, Figure 5d; Surkova et al., 2013, Figure S7). L2 has altered expression in a subset of the stripe 4–6 region, increased amplitude of stripe 3 expression early, and a reduction in stripe 5 expression before T6, similar to that seen in *kni*/+. The deletion in L2 comprises 30% of the kni_+1 enhancer, which drives expression in both the head and putative abdomen (Schroeder et al., 2004). The L2 deletion also removes sequences in the kni proximal shadow enhancer (Perry et al., 2011). These observations led us to predict that Kni expression would be reduced in L2.

We tested our prediction by performing antibody staining of Kni in two independent experiments: L1 versus L2 and L2 versus L5. In each of these experiments, we compared embryos in early (T2–T3), middle (T4–T6), and late (T7–T8) cleavage cycle 14A. In early cleavage cycle 14A Kni expression is consistently lower in L2 than either L1 or L5 (Wilcoxon rank sum test of peak height between 45% and 80% AP position gives $p = 0.0001$ for L1 versus L2, and $p = 1.8 \times 10^{-6}$ for L2 versus L5; see Fig. 4). In mid to late cycle 14A, L2 and L5 show indistinguishable levels of Kni expression, but

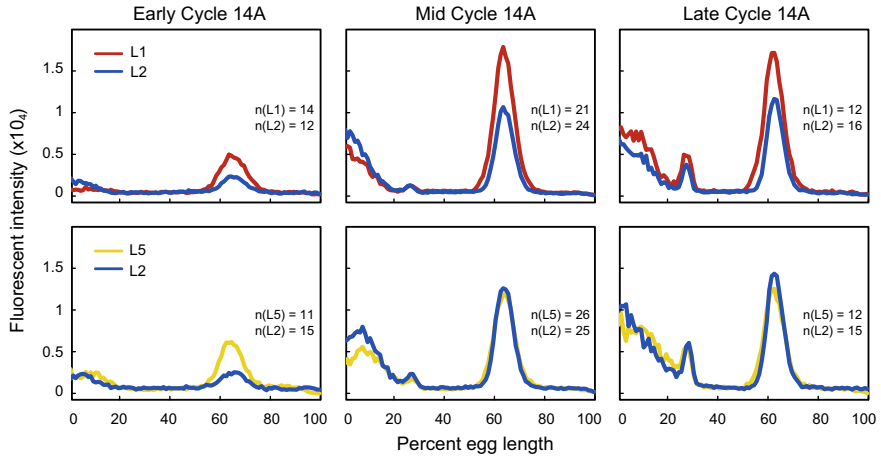

Fig. 4. Knirps expression in three lines. Average 1D Kni protein expression in three lines determined by two antibody staining experiments: L1 versus L2 and L2 versus L5 (upper and lower panel respectively). Expression from the middle 10% of D-V coordinates of laterally oriented embryos is shown. The early cycle 14A temporal class comprises T2 and T3, the mid-cycle 14A temporal class comprises T4, T5 and T6, and the late cycle 14A temporal class comprises T7 and T8. Axes are as labeled; the numbers of embryos imaged in each time class are shown.

L1 gives slightly higher expression than the other two lines. There exist multiple lines of evidence that the time of formation of *eve* stripes is determined by rising levels of repressive gap gene products (Stanojevic et al., 1991; Small et al., 1992; Reinitz and Sharp, 1995; Fujioka et al., 1999; Janssens et al., 2006; Surkova et al., 2008), and hence it is extremely likely that the *kni* deletion in L2 is responsible for the *eve* phenotype we observe.

Only L2 bears this deletion among the DGRP collection of approximately 200 lines. In the core DPGP2 lines (Pool et al., 2012), which consist of lines originating from African and a few European populations, the full deletion is absent, although two small deletions (7–8 bp each) segregate in these populations. The 448 bp deletion in L2 may, therefore, be a low frequency variant with limited geographic range.

3. Discussion

The three lines displayed three distinct *eve* stripe expression patterns. This variability was large enough to depart from the evolutionarily conserved reference pattern. The overall higher expression of *eve* in L5 could be caused by genetic variants controlling overall *eve* expression. In *cis*, these might involve variants in the *eve* autoregulatory elements or some unknown chromatin regulation mechanism at the whole-locus level. In *trans*, the cause could be the consequence of expression level changes of other genes in the network. In the absence of a clear genomic signature, further experimentation will be required to elucidate the cause of increased expression. In addition to the higher overall expression of *eve* in L5, we observed in L2 the absence of *eve* stripe 5 formation at T4, the time at which stripe 5 typically becomes visible (Surkova et al., 2008). Although the seven-stripe pattern is restored in the blastoderm embryo by T6, alternations in interstripe distances persist well into gastrulation. These differences are consistent from embryo to embryo, and are supported by relatively conservative statistical methods that do not assume normality and take into account multiple pairwise tests of significance. The unusual early *eve* expression pattern has measurable consequences later in the pattern formation cascade, as evidenced by a significant change in the spacing of En stripes. The altered pattern of *eve* expression in L2 strongly resembles that seen in a *kni* heterozygote (Surkova et al., 2013), and we found that this line bears a 448 bp deletion in its *kni* intron, which removes part of the kni_+1 enhancer. This mutation appears to be rare in *D. melanogaster*, as it is not present in any other DGRP line, nor in any DPGP2 line, the majority of which are African lines representing the ancestral range of that species.

We predicted that this deletion would lead to reduced *kni* expression, and verified this prediction by quantitative measurement of Kni expression. These observations strongly suggest the contribution of the *trans* background to *eve* stripe variation.

Odd numbered *en* stripes are expressed at the anterior margin of *eve* stripes, while the even numbered stripes are expressed at the anterior margins of *ftz* stripes (Hughes and Krause, 2001). The expansion of the 3/4 *eve* interstripe leads to an increase of the distance between *en* stripes 6 and 7. The position of *en* stripe 6 relative to 5 and 7 depends on *ftz* expression (Hughes and Krause, 2001; Fujioka et al., 1995) and may indicate that *ftz* stripes are also altered in L2. Similarly, the reduction in the length of the *eve* 4/5 early interstripe causes a decrease in the total distance between the *eve*-dependent *en* stripes 7 and 9. The effect of the reduction of stripe 5 expression on parasegment 9 (the distance between *en* stripes 9 and 10) is reminiscent of that seen in enhancer deletions, but much milder (Fujioka et al., 2002). This effect is also consistent with observations of *ftz* expression in *kni* heterozygotes (Carroll et al., 1988, Figure 3F). In these embryos, *ftz* stripes 4 and 5 are markedly closer, consistent with reduction in distance between *en* stripes 8 and 10, while the distance between *ftz* stripes 3 and 4 increases, implying an increase of distance between *en* stripes 6 and 8.

In *kni* and *Kr* heterozygotes, altered gap and pair-rule expression are largely corrected by gastrulation (Surkova et al., 2013). In L2 we did observe an En expression phenotype attributable to *eve* misexpression, but adults do not display any obvious phenotypic defect, and the line is viable and fertile. In *bicoid* copy number variants, the expansion of the head region in flies with extra *bicoid* copies is corrected by differential cell apoptosis (Busturia and Lawrence, 1994; Namba et al., 1997). Multiple layers of canalization may buffer misexpression of early genes in the segmentation pathway, making variations more common than previously suspected based on the strong evolutionarily conservation of the pathway. Canalization theory predicts such variation in strongly buffered pathways (Meiklejohn and Hartl, 2002).

3.1. Evolutionary implications

The most surprising result reported here is that phenotypic variation in *eve* expression within *D. melanogaster* is of larger

magnitude than previously reported inter-species variation between *D. melanogaster* and *D. pseudoobsecura*. We believe that *eve* expression is under relatively strong stabilizing selection, and therefore it is generally conserved across relatively large evolutionary distance. However, the large variation within species indicates that conservation is not complete, and that there is a large potential for expression to change. There must be limits to natural variation, however, and the fact that the *kni* deletion is a rare variant suggests that it is deleterious in nature. The similarity of the L2 *eve* phenotype to that of *kni* heterozygote mutant embryos, which are viable, suggests that the permissive threshold may be around half of wild type expression. In natural populations, the *kni* deletion variant will be present almost entirely in heterozygotes because it is rare, and we expect that the phenotypic effect in heterozygotes will be subtler than the homozygous effects measured in L2.

Examples of *cis* and *trans* coevolution are pervasive (Barrière and Ruvinsky, 2014; Gordon and Ruvinsky, 2012; Ludwig et al., 2005), and binding sites turnover, rearrangement, and change of spacing within enhancers is rampant for phenotypically conserved traits. Both may be manifestations of compensatory evolution. There are also examples of developmental system drift (True and Haag, 2001), in which the underlying genetic network changes over evolutionary time while maintaining a specific phenotype. However, no detailed mechanism has been proposed for that phenomenon. Our work suggests that canalization of mutant phenotypes compresses the width of their phenotypic distribution. This reduces the consequences of genetic variance, allowing otherwise dramatic mutations, such as the partial loss of the kni_+1 enhancer, to segregate in natural populations for a long enough time without being eliminated by selection to allow other compensatory mutations to occur. A computational model of enhancer evolution under stabilizing selection (Bullaughey, 2011) predicts rapid turnover of binding sites, and in many cases deleterious mutations persist before positive selection takes place. Buffering mechanisms will greatly reduce the fitness cost of a deleterious mutation, and therefore greatly increase the rate of compensatory evolution (Durrett and Schmidt, 2008). Canalization, compensatory evolution, and developmental system drift may be multiple consequences of stabilizing selection acting to maintain the fidelity of developmental processes.

Variation in spatio-temporal patterns of gene expression in conserved developmental systems, as described in this work, is likely to be widespread as a consequence of buffering mechanisms that mitigate their developmental consequences on adult fitness. We note that strongly deleterious mutations, though rare in their individual frequency, are numerically abundant (though absent in the inbred DGRP lines). The *kni* deletion mutant may be an example of a non-lethal deleterious allele exhibiting a dramatic molecular phenotype. Deleterious mutations with molecular phenotype are expected to be much more common in natural populations than in the DGRP lines. We might also anticipate finding some of these variants to be common in populations if they co-occur with compensatory mutations. The continued development of models of transcription, such as Kim et al. (2013), will be useful for predicting the effects of natural variation on gene expression.

4. Materials and methods

4.1. Fly culture, embryo collection and fixation

Flies were grown and embryos were collected at 25 °C. For *eve in situ* hybridization and antibody staining, embryos were collected after 1.5 h, and aged for another 2 h. Fixation was performed as described (Kosman et al., 2004) with a fixation time of 25 min. En antibody staining was performed on embryos aged for 8 h and fixed for 10 min.

4.2. Fluorescent in situ hybridization and antibody staining

Fluorescent *in situ* hybridization followed the published protocol (Kosman et al., 2004). FITC-labeled *eve* antisense RNA probe was generated from p48-X1.4 (Macdonald et al., 1986) using SP6 polymerase. Following hybridization, embryos were incubated with rabbit anti-FITC (1:1000) and Guinea Pig (1:1000) anti-Eve antibody (Azpiazu and Frasch, 1993). After washing, embryos were incubated in Alexa Fluor 647 Goat Anti-Rabbit IgG (Life Technologies, 1:1000) and Alexa Fluor 555 Goat Anti-Guinea Pig IgG (Life Technologies, 1:1000). Nuclei were stained with DAPI (Life Technologies Cat. No. P36935). En protein is stained with mouse MAb 4D9 antibody (1:3) followed by Goat Anti-Mouse IgG-HRP (1:300) (Patel, 1994). For Kni staining, embryos were incubated with anti-Kni Guinea Pig antibody (1:1000), followed by Alexa Fluor 555 Goat Anti-Guinea Pig IgG (1:1000) and anti-Eve Rabbit (1:2000) followed by Alexa Fluor 647 Goat Anti-Rabbit IgG (1:1000).

4.3. Imaging

Fluorescence data was acquired on a Leica SP5 confocal microscope. Gain was set to produce several saturated pixels after averaging, and offset was set so that approximately half of the background pixels outside the embryo displayed zero intensity and half non-zero intensity. This procedure was carried out with the 5 brightest embryos for each line, and the setting for the brightest line was used to standardize all data collection. Images were taken from the surface of lateral embryos, using a 20X apo objective (HC PL APO 20x/0.70NA lens [dry]). The images for *eve* are 12 bits per pixel and have 8 line averages. Note that 12 bit images are converted to 16 bit during processing, so that the fluorescent intensity is of 16 bit range. Five *z*-sections of 0.5 μm each were acquired for laterally oriented embryos. From these five *z*-sections, the three that best traverse the layer of blastoderm nuclei that is close to cover slide were selected for further processing. A DIC image of the middle of the embryo was acquired to visualize membrane invagination to aid in time classification. Images for Kni staining were acquired under the same microscope, with 8 bit depth (converted to 16 bit showing in graph), two *z*-sections which are 1 μm apart.

Images of En staining were acquired using Zeiss Axioskop light microscope.

4.4. Time classification

Time classification of younger (T1–T3) embryos was performed by inspection of protein expression patterns as described by Surkova et al. (2008). Older (T4–T8) embryos were categorized by the degree of cell membrane invagination. We noticed the membrane at the ventral side is more mature than the dorsal side, and we based on our membrane invagination on the ventral side membrane. The time classification by membrane invagination is quite robust, while the early patterns are not as reliable. For T1–T3 embryos, we noticed that characteristic stages of the RNA pattern occur about one time class earlier than the same stage of the protein pattern. This fact was useful in the classification of the altered patterns seen in some lines. T1 embryos could always be unambiguously classified by protein pattern. The RNA patterns of these embryos were indicative of the expected T2 protein pattern of a particular line. Continuation of this procedure provided consistent and reliable temporal classification for all lines.

4.5. Feature detection

For observations of *eve* and Kni expression, segmentation, background removal, and the extraction of data from the central 10% of dorso-ventral positional values were performed as described by Surkova et al. (2008). Embryos stained for Kni were registered using Eve stripes as described by Surkova et al. (2008). For investigations of *eve* expression, cubic splines were used to detect extrema and borders of the stripes for time class T4–T8, when all seven *eve* stripes are detectable (Ludwig et al., 2011). A border is defined to be the position with expression midway between that of a stripe peak and interstripe. Each stripe, except 1 and 7, has an anterior and posterior height defined by the difference between expression at the stripe peak and the adjacent interstripe. The width of a stripe was taken to be the distance between its borders in percent egg length (% EL), with 0% at the anterior pole. A small number of embryos that were detected to have fewer or more than the full set of 13 extrema were included in the analysis after manual addition or removal of extraneous features. The number of embryos collected for each time class is summarized in Supplementary Table S6.

4.6. Measurement of En parasegments

Points were marked at the midline of the anterior of each En stripe using imageJ (Schneider et al., 2012) (see the red dots in Fig. 3A), and parasegment lengths were measured between these points. The normalized parasegment length was taken to be the length of each parasegment divided by the sum of length from all the parasegments in that embryo.

4.7. Measurement of embryo size

In the data processing step, we generate an outline of the entire embryo with the length in pixels of the major and minor axes. These are converted to microns using metadata from confocal imaging.

4.8. PCR primers

For validation of deletions for

eve: forward:GGTCGCTTGGAGAAGGAGTT reverse: CACACCCAGTCCGGTATAGC
gt: forward: TGGCACAAGAGCTCGATGTT reverse: TAAATGCAGGGGGTTCCGAC
kni: forward: CCTAAGTGTGAGCGAGCACA reverse: TGAGAAAACGTGCAGCAACG
runt: forward:ACATGACCTACGGCTATGCG reverse: TAATTTTTGCCCGCTTGCCG

Acknowledgments

We thank Chun Wai Kwan, Ah-Ram Kim, Hilde Janssens, Kenneth Barr, Vytas Bindokas, Stephen Small, Maira Arruda Cardoso, Ziyue Gao and Mengyu Xu for useful discussions and help. The work is supported by NIH Grant NIH R01 OD010936 (formerly RR07801), and the University of Chicago. Imaging was performed at the University of Chicago Integrated Light Microscopy Facility.

Appendix A. Supplementary data

Supplementary data associated with this article can be found in the online version at http://dx.doi.org/10.1016/j.ydbio.2015.06.019.

References

Arnosti, D.N., Barolo, S., Levine, M., Small, S., 1996. The eve stripe 2 enhancer employs multiple modes of transcriptional synergy. Development 122, 205–214.
Azpiazu, N., Frasch, M., 1993. *tinman* and *bagpipe*: two homeo box genes that determine cell fates in the dorsal mesoderm of *Drosophila*. Genes Dev. 7, 1325–1340.
Barrière, A., Ruvinsky, I., 2014. Pervasuve divergence of transcriptional gene regulation in Caenorhabditis Nematodes. PLoS Genet. 10, e1004435.
Barrière, A., Gordon, K.L., Ruvinsky, I., 2011. Distinct functional constraints partition sequence conservation in a *cis*-regulatory element. PLoS Genet. 7, e1002095.
Bullaughey, K., 2011. Changes in selective effects over time facilitate turnover of enhancer sequences. Genetics 187, 567–582.
Bullock, S.L., Stauber, M., Prell, A., Hughes, J.R., Ish-Horowicz, D., Schmidt-Ott, U., 2004. Differential cytoplasmic mRNA localisation adjusts pair-rule transcription factor activity to cytoarchitecture in dipteran evolution. Development 131, 4251–4261.
Busturia, A., Lawrence, P.A., 1994. Regulation of cell number in *Drosophila*. Nature 370, 561–563.
Carroll, S.B., Laughon, A., Thalley, B.S., 1988. Expression, function and regulation of the *hairy* segmentation protein in the *Drosophila* embryo. Genes Dev. 2, 883–890.
Davis, G.K., Patel, N.H., 2002. Short, long, and beyond: molecular and embryological approaches to insect segmentation. Ann. Rev. Entomol. 47, 669–699.
Durrett, R., Schmidt, D., 2008. Waiting for two mutations: with applications to regulatory sequence evolution and the limits of Darwinian evolution. Genetics 180, 1501–1509.
Fisher, S., Grice, E.A., Vinton, R.M., Bessling, S.L., McCallion, A.S., 2006. Conservation of RET regulatory function from human to zebrafish without sequence similarity. Science 312, 276–279.
Fowlkes, C.C., Eckenrode, K.B., Bragdon, M.D., Meyer, M., Wunderlich, Z., Simirenko, L., et al., 2011. A conserved developmental patterning network produces quantitatively different output in multiple species of *Drosophila*. PLoS Genet. 7.
Frasch, M., Levine, M., 1987. Complementary patterns of *even-skipped* and *fushi-tarazu* expression involve their differential regulation by a common set of segmentation genes in *Drosophila*. Genes Dev. 1, 981–995.
Fujioka, M., Jaynes, J.B., Goto, T., 1995. Early *even-skipped* stripes act as morphogenetic gradients at the single cell level to establish *engrailed* expression. Development 121, 4371–4382.
Fujioka, M., Emi-Sarker, Y., Yusibova, G.L., Goto, T., Jaynes, J.B., 1999. Analysis of an *even-skipped* rescue transgene reveals both composite and discrete neuronal and early blastoderm enhancers, and multi-stripe positioning by gap gene repressor gradients. Development 126, 2527–2538.
Fujioka, M., Yusibova, G.L., Patel, N.H., Brown, S.J., Jaynes, J.B., 2002. The repressor activity of Even-skipped is highly conserved, and is sufficient to activate engrailed and to regulate both the spacing and stability of parasegment boundaries. Development 129, 4411–4421.
Gallo, S.M., Gerrard, D.T., Miner, D., Simich, M., Des Soye, B., Bergman, C.M., Halfon, M.S., 2011. REDfly v3.0: toward a comprehensive database of transcriptional regulatory elements in *Drosophila*. Nucleic Acids Res. 39, D118–D123.
Gilbert, S.F., 2003. Developmental Biology, seventh ed. Sinauer Associates, Sunderland, MA.
Gordon, K.L., Ruvinsky, I., 2012. Tempo and mode in evolution of transcriptional regulation. PLoS Genet. 8, e1002432.
Goto, T., MacDonald, P., Maniatis, T., 1989. Early and late periodic patterns of *even-skipped* expression are controlled by distinct regulatory elements that respond to different spatial cues. Cell 57, 413–422.
Gregor, T., Tank, D.W., Wieschaus, E.F., Bialek, W., 2007. Probing the limits to positional information. Cell 130, 153–164.
Harding, K., Hoey, T., Warrior, R., Levine, M., 1989. Autoregulatory and gap gene response elements of the *even-skipped* promoter of *Drosophila*. EMBO J. 8, 1205–1212.
Hare, E.E., Peterson, B.K., Iyer, V.N., Meier, R., Eisen, M.B., 2008. Sepsid even-skipped enhancers are functionally conserved in *Drosopila* despite lack of sequence conservation. PLoS Genet. 4, e1000106.
Houchmandzadeh, B., Wieschaus, E., Leibler, S., 2002. Establishment of developmental precision and proportions in the early *Drosophila* embryo. Nature 415, 798–802.
Hughes, S.C., Krause, H.M., 2001. Establishment and maintenance of parasegmental compartments. Development 128, 1109–1118.
Janssens, H., Kosman, D., Vanario-Alonso, C.E., Jaeger, J., Samsonova, M., Reinitz, J., 2005. A high-throughput method for quantifying gene expression data from early *Drosophila* embryos. Dev. Genes Evol. 215, 374–381.
Janssens, H., Hou, S., Jaeger, J., Kim, A.R., Myasnikova, E., Sharp, D., Reinitz, J., 2006. Quantitative and predictive model of transcriptional control of the *Drosophila melanogaster even skipped* gene. Nat. Genet. 38, 1159–1165.
Karolchik, D., Barber, G.P., Clawson, H., Cline, M.S., Diekhans, M., et al., 2014. The UCSC Genome Browser database: 2014 update. Nucleic Acids Res. 42, D764–D770.
Kent, W.J., 2002. Blat—the blast-like alignment tool. Genome Res. 12, 656–664.
Kim, A.R., Martinez, C., Ionides, J., Ramos, A.F., Ludwig, M.Z., Ogawa, N., Sharp, D.H., Reinitz, J., 2013. Rearrangements of 2.5 kilobases of noncoding DNA from the *Drosophila even-skipped* locus define predictive rules of genomic *cis*-regulatory logic. PLoS Genet. 9, e1003243.
Kosman, D., Mizutani, C.M., Lemons, D., Cox, W.G., McGinnis, W., Bier, E., 2004.

Multiplex detection of RNA expression in *Drosophila* embryos. Science 305, 846.
Larkin, M.A., Blackshields, G., Brown, N.P., Chenna, R., McGettigan, P.A., McWilliam, H., Valentin, F., Wallace, I.M., Wilm, A., Lopez, R., Thompson, J.D., Gibson, T.J., Higgins, D.G., 2007. Clustal W and clustal X version 2.0. Bioinformatics 23, 2947–2948.
Lott, S.E., Kreitman, M., Palsson, A., Alekseeva, E., Ludwig, M.Z., 2007. Canalization of segmentation and its evolution in *Drosophila*. Proc. Natl. Acad. Sci. U.S.A. 104, 10926–10931.
Ludwig, M.Z., Patel, N.H., Kreitman, M., 1998. Functional analysis of *eve* stripe 2 enhancer evolution in *Drosophila*: rules governing conservation and change. Development 125, 949–958.
Ludwig, M.Z., Palsson, A., Alekseeva, E., Bergman, C.M., Nathan, J., Kreitman, M., 2005. Functional evolution of a *cis*-regulatory module. PLoS Biol. 3 (4), e93.
Ludwig, M.Z., Manu, Kittler, R., White, K.P., Kreitman, M., 2011. Consequences of eukaryotic enhancer architecture for gene expression dynamics, development, and fitness. PLoS Genet. 7, e1002364.
Macdonald, P.M., Ingham, P., Struhl, G., 1986. Isolation, structure, and expression of *even-skipped*: a second pair-rule gene of *Drosophila* containing a homeo box. Cell 47, 721–734.
Mackay, T.F.C., Richards, S., Stone, E.A., et al., 2012. The *Drosophila melanogaster* genetic reference panel. Nature 482, 173–178.
Manu, Surkova, S., Spirov, A.V., Gursky, V., Janssens, H., Kim, A., Radulescu, O., Vanario-Alonso, C.E., Sharp, D.H., Samsonova, M., Reinitz, J., 2009. Canalization of gene expression in the *Drosophila* blastoderm by gap gene cross regulation. PLoS Biol. 7, e1000049.
Manu, Ludwig, Michael Z., Kreitman, Martin, 2013. Sex-specific pattern formation during early *Drosophila* development. Genetics 194, 163–173.
Martinez, Carlos, Kim, Ah-Ram, Rest, Joshua S., Ludwig, Michael, Kreitman, Martin, White, Kevin, Reinitz, John, 2014. Ancestral resurrection of the *Drosophila* S2E enhancer reveals accessible evolutionary paths through compensatory change. Mol. Biol. Evol. 31, 903–916.
Meiklejohn, C.D., Hartl, D.L., 2002. A single mode of canalization. Trends Ecol. Evol. 17 (10), 468–473.
Miles, C.M., Lott, S.E., Luengo Hendriks, C.L., Ludwig, M.Z., Manu, Williams, C.L., Kreitman, M., 2011. Artificial selection on egg size perturbs early pattern formation in *Drosophila melanogaster*. Evolution 65, 33–42.
Namba, R., Pazdera, T.M., Cerrone, R.L., Minden, J.S., 1997. *Drosophila* embryonic pattern repair: how embryos respond to *bicoid* dosage alternation. Development 124, 1393–1403.
Nüsslein-Volhard, C., Wieschaus, E., 1980. Mutations affecting segment number and polarity in *Drosophila*. Nature 287, 795–801.
Palsson, A., Wesolowska, N., Reynisdóttir, S., Ludwig, M.Z., Kreitman, M., 2014. Naturally occurring deletions of hunchback binding sites in the *even-skipped* stripe 3+7 enhancer. PLoS ONE 9, e91924.
Patel, N.H., 1994. Imaging neuronal subsets and other cell types in whole-mount *Drosophila* embryos and larvae using antibody probes. Methods Cell Biol. 44, 445–487.
Perry, M., Boettiger, A.N., Levine, M., 2011. Multiple enhancers ensure precision of gap gene-expression patterns in the *Drosophila* embryo. Proc. Natl. Acad. Sci. U.S.A. 108, 13570–13575.
Pool, J.E., Corbett-Detig, R.B., Sugino, R.P., Stevens, K.A., Cardeno, C.M., Crepeau, M.W., Duchen, P., Emerson, J.J., Saelao, P., Begun, D.J., Langley, C.H., 2012. Population Genomics of sub-saharan *Drosophila* melanogaster: African diversity and non-African admixture. PLoS Genet. 8, e1003080.
Reinitz, J., Sharp, D.H., 1995. Mechanism of *eve* stripe formation. Mech. Devel. 49, 133–158.
Richards, S., Liu, Y., Bettencourt, B.R., et al., 2005. Comparative genome sequencing of *Drosophila pseudoobscura*: chromosomal, gene, and *cis*-element evolution. Genome Res. 15, 1–18.
Romano, L.A., Wray, G.A., 2003. Conservation of Endo16 expression in sea urchins despite evolutionary divergence in both *cis* and *trans*-acting components of transcriptional regulation. Development 130, 4187–4199.
Schneider, C.A., Rasband, W.S., Eliceiri, K.W., Schindelin, J., Arganda-Carreras, I., et al., 2012. NIH image to ImageJ: 25 years of image analysis. Nat. Methods 9, 671–675.
Schroeder, M.D., Pearce, M., Fak, J., Fan, H.-Q., Unnerstall, U., Emberly, E., Rajewsky, N., Siggia, E.D., Gaul, U., 2004. Transcriptional control in the segmentation gene network of *Drosophila*. PLoS Biol. 2, e271.
Small, S., Blair, A., Levine, M., 1992. Regulation of even-skipped stripe 2 in the *Drosophila* embryo. EMBO J. 11, 4047–4057.
Small, S., Arnosti, D.N., Levine, M., 1993. Spacing ensures autonomous expression of different stripe enhancers in the *even-skipped* promoter. Development 119, 767–772.
Small, S., Blair, A., Levine, M., 1996. Regulation of two pair-rule stripes by a single enhancer in the *Drosophila* embryo. Dev. Biol. 175, 314–324.
Stanojevic, D., Small, S., Levine, M., 1991. Regulation of a segmentation stripe by overlapping activators and repressors in the *Drosophila* embryo. Science 254, 1385–1387.
Surkova, S., Kosman, D., Kozlov, K., Manu, Myasnikova, E., Samsonova, A., Spirov, A., Vanario-Alonso, C.E., Samsonova, M., Reinitz, J., 2008. Characterization of the *Drosophila* segment determination morphome. Dev. Biol. 313 (2), 844–862.
Surkova, S., Golubkova, E., Manu, Panok, L., Mamon, L., Reinitz, J., Samsonova, M., 2013. Quantitative dynamics and increased variability of segmentation gene expression in the *Drosophila Krüppel* and *knirps* mutants. Dev. Biol. 376, 99–112.
True, J.R., Haag, E.S., 2001. Developmental system drift and flexibility in evolutionary trajectories. Evol. Dev. 3, 109–119.
Waddington, C.H., 1942. Canalization of development and the inheritance of acquired characters. Nature 150, 563–565.